DEUTSCHES ELEKTRONEN-SYNCHROTRON DESY

DESY 70/47
September 1970

OPTICAL ABSORPTION OF SOLID NEON AND ARGON IN THE SOFT X-RAY REGION

by

R. Haensel, G. Keitel, N. Kosuch, U. Nielsen and P. Schreiber

Deutsches Elektronen-Synchrotron DESY, Hamburg, Germany

and

II. Institut für Experimentalphysik der Universität Hamburg,

Hamburg, Germany

2 HAMBURG 52 · NOTKESTIEG 1

Optical Absorption of Solid Neon and Argon in the Soft X-Ray Region

R. Haensel, G. Keitel, N. Kosuch, U. Nielsen and P. Schreiber

Deutsches Elektronen-Synchrotron, Hamburg, Germany

and

II. Institut für Experimentalphysik der Universität Hamburg,

Hamburg, Germany

The absorption spectra of thin films of solid Ne and Ar have been measured in the photon energy range 25 to 500 eV. For comparison with the atomic states the corresponding spectra in the gas have also been investigated. The 7.5 GeV electron synchrotron DESY served as light source. Near the onset of inner shell transitions (2s in Ne, 3s and 2s in Ar) fine structure can be seen which is characteristic for the solid or atomic state. The structure in the spectra of the solid is ascribed to exciton and interband transitions. The absorption in the continuum at some distance from the various thresholds shows great similarities between the solid and gaseous states.

I. INTRODUCTION

The solid rare gases which crystallize in the fcc lattice structure are among the simplest solids. While the lattice structure and dynamics have been investigated to some extent[1,2], only some measurements have been performed on the optical properties.

Most measurements of the optical constants cover only the fundamental absorption region. Optical absorption measurements extend up to 14 eV[3-6], whereas optical reflection[7-11] and electron energy loss measurements[12-15] extend to about 30 eV.

At the onset of optical absorption, lines are observed the energy positions of which are very close to the first resonance absorption lines in the gases (8.43 eV in Xe, 10.03 eV in Kr, 11.62 eV in Ar and 16.68 eV in Ne[16]). These lines are normally interpreted as an intermediate case of Frenkel and Wannier excitons[17]. The first few absorption lines form a hydrogenlike series converging to the onset of interband transitions. The absorption structures due to interband transitions can be discussed in the light of recent energy band calculations[18-25].

Going to higher energies the absorption coefficient generally decreases monotonically with less structure up to the energy where transitions from core shells become possible. In the atomic state the absorption lines due to transitions from the different inner shells have been extensively studied up to 150 eV by means of synchrotron radiation at the NBS[26-28]. Many measurements have also been performed on the continuum absorption between thresholds, where the transition matrix element[29-31] mainly determines the shape of the absorption continuum.

As the rare gases have been extensively investigated in the atomic state both experimentally and theoretically they are ideally suited for a comparison of the absorption cross sections of one material in both the gaseous and solid states.

Measurements of core transitions in solid Kr (3d) and Xe (4d) have recently been performed at DESY in the energy range up to 500 eV[32-34]. They have shown that near threshold the absorption spectra show big differences between the gaseous and solid state; for energies of 10 eV or more above threshold the spectra in both states are more and more alike, so that the atomic calculations also are a good approximation for the solid state.

In the following sections we want to report on measurements which have been performed on gaseous and solid Ne and Ar in the energy range 25 to 500 eV. This energy range covers the onset of transitions from the 2s-shell in Ne and from the 3s, 2p and 2s shell in Ar. Data of the line shape of 2s-transitions in Ne and 3s-transitions in Ar have already been reported in a previous paper[35]. Section II will give a short description of the experimental procedure and section III will present and discuss the experimental results.

II. EXPERIMENTAL PROCEDURE

Of the three different techniques used for the measurement of the optical constants of the solid rare gases in the fundamental absorption region, only thin film absorption can be used in the 25 to 500 eV range. The optical normal-incidence reflectivity is very small (< 0.01). Therefore, the error due to long wavelength stray light, which is reflected with a much higher reflectivity, is not tolerable. Electron energy loss measurements do not give sufficient energy resolution in this spectral range.

The experimental arrangement (Fig. 1) is the same as has been used for the Kr and Xe measurements[33,34]. Light is coming from the 7.5 GeV electron synchrotron DESY[36,37]. The thin films of solid Ne and Ar were evaporated onto thin C- or Al-foils, mounted in a cryostat with variable temperature. Contamination of the samples was avoided by a shield with tubular extensions into both sides of the beam pipe which were cooled to liquid N_2-temperature. The spectrometer is a 1 m Rowland mounting with gratings G of 2400 lines/mm and 3600 lines/mm. The energy resolution was better than 0.1 Å. By choosing appropriate angles of incidence onto the grating, and by the use of a premirror M in front of the entrance slit ES and of Al-, Mg- and Sb-filters F, light of higher order reflections of the grating and stray light is essentially suppressed[38]. The energy calibration is based on the energy positions of gas absorption lines of Ne[27] and Ar[28] as given by Madden et al. For the gas absorption measurements, the cryostat is replaced by a gas absorption cell[39] with C- or Al-windows. The gas pressure is measured by a precision membrane vacuum meter (Datametrics Model 1014).

The absolute accuracy of the absorption coefficient obtained in our measurements is 15 % in the energy range 40 eV to 280 eV, and 30 % elsewhere. The relative accuracy was much better, differences in the absorption coefficient in the order of 1 % were clearly detectable if photon energies were not more than some eV apart.

III. EXPERIMENTAL RESULTS AND DISCUSSION

A. Continuum Absorption

The absorption cross section σ of solid and gaseous Ne is shown in Fig. 2. Our gas measurements (dashed line) range from 110 to 280 eV. For comparison

results of other authors[40-44] are included. They are in good agreement with our results. The absorption coefficient for solid Ne (solid line) has been measured from 25 to 400 eV. As the thickness of the solid Ne film has not been determined directly the absorption coefficient of the solid is only known in arbitrary units. The adjustment is made by setting equal the integrated oscillator strengths of the solid and of the gas over the whole spectral range. By doing so we see an excellent agreement of both curves. This procedure has previously been applied with good success to Kr and Xe[33,34]. On the basis of a lattice constant of 4.46 Å (fcc lattice)[1] the value of the exponential absorption coefficient μ for solid Ne is given on the right-hand scale.

Figure 3 shows the absorption curves for Ar. The gas measurements (dashed line) range from 90 eV to 400 eV. For comparison results of other authors[28,41,43-49] are included. They are in good agreement with our results. The absorption coefficient of solid Ar (solid line) has been measured from 25 to 500 eV. The film thickness has not been measured directly and the normalisation has been made by setting equal the integrated oscillator strength of gaseous and solid Ar. On the basis of a lattice constant of 5.31 Å (fcc lattice)[1] the value for the exponential absorption coefficient μ is given for solid Ar on the right-hand scale.

We see that the overall behaviour of the absorption cross section of solid Ne and Ar can be described by the atomic approximation. In the X-ray range the energy dependence of the absorption coefficient can normally be described by an hydrogen-like behaviour as

$$\sigma(E) = \text{const.}\ E^{-\alpha} \quad (\alpha = \text{const}) \tag{1}$$

excluding the vicinity above thresholds for inner shell excitations, where the fine structure occurs.

In Ar one sees at 250 eV clearly the onset of 2p-transitions and the decrease of the absorption coefficient according to Eq. (1), beginning at some ten eV above the 2p-threshold. For the 3p-transitions of Ar (threshold at ∿ 16 eV) and the 2p-transitions of Ne (threshold at ∿ 21 eV), however, the hydrogen-like behaviour according to Eq. (1) is only observable at energies > 150 eV. In the immediate vicinity of the thresholds the absorption is suppressed and delayed due to the balance between Coulomb potential and the $l(l+1)/r^2$ term in the radial wave equation of the atom[29-31].

The striking difference of the 3p-spectrum in Ar compared with the 2p-spectra in Ar and Ne is the occurrence of the absorption minimum at 49 eV, which is followed by a maximum at 80 eV. This feature is connected with the so-called resonance near threshold[31]. It has been found to occur generally in the case of transitions from initial states in outer shells whose wave functions have nodes. (Therefore, the 2p-transitions do not show a minimum). Since in this case the overlapping integral between initial and final state wave functions is always negative at threshold and positive at energies far above threshold, the matrix-element has to change sign at an intermediate energy. For Ar 3p→d transitions this occurs near 50 eV, leading to the minimum of the absorption coefficient.

B. Fine Structure

Neon

Figure 4 shows details of the Ne spectrum in Fig. 2 between 25 and 70 eV. The asymmetric lines in the spectrum of gaseous Ne are due to 2s→np transitions. We have not measured the gas pressure in this case. The curve was fitted to Samson's values[40]. The spectrum of the solid shows asymmetric absorption lines[35], but they are broader and are shifted to higher energies in comparison with the

gas lines. Below 45 eV, where the gas spectrum is flat, many structures can be seen in the spectrum of the solid. They are obviously due to transitions from the valence band and caused by the density of states of the conduction band. It is not clear whether the structure above 50 eV is also due to 2p- or to 2s-transitions. A detailed discussion of the 2p-transition structure in view of recent energy band calculations by Rössler[25] is beyond the scope of this paper.

Argon

In Fig. 3 one sees window lines in the absorption curves[35] of solid Ar near 27 eV, where Madden et al.[28] have found lines of similar shape for gaseous Ar. As in Ne, the general character of the Ar lines is preserved but they are broadened and shifted to higher energies. These lines are ascribed to 3s→np transitions.

Figure 5 shows the fine structure of the 2p-transitions above 245 eV[50]. The absorption spectrum of gaseous Ar (dashed curve) is in agreement with other measurements[46,51-53]. The absorption lines can be ascribed to 2p→ns,nd transitions, with corresponding peaks separated by the energy distance of the 2p spin-orbit splitting of the core state (2.03 eV).

The absorption spectrum of solid Ar (solid line) also shows many absorption peaks. Corresponding spin-orbit partners are labeled with primed and unprimed capital letters.

Additionally the absorption spectra of different Ar-N_2 alloys have been measured. If one adds N_2 to Ar, the peaks B, B', E, D' etc. are broadened and shifted to higher energies. In a mixture of Ar : N_2 = 1 : 9 the shift of B and B' to higher energies is 1 eV against the position in pure Ar. The peaks A and A' are not

affected by alloying with N_2, i. e. the double peak A'B in pure Ar is clearly separated into two peaks in the Ar-N_2 alloy.

From this behaviour we conclude that all peaks except of A and A' depend on the variation of the density of states of the conduction band. We assume that the peaks A and A' are Frenkel excitons, since they are not affected by the alloying and since they have their energy position and oscillator strength close to that of the first gas absorption lines (2p→4s).

As peak B is shifted to higher energies in the Ar-N_2 alloys, a small shoulder appears at about 246 eV. This could be due either to higher ($n \geq 2$) members of the exciton series or to the onset of interband transitions. In any case the threshold for 2p interband transitions is expected to lie at about 246 eV. For a comparison with the 3p-transition we have separated the two components in the 2p absorption of solid Ar in such a way that only the contribution of one of the two spin orbit split 2p-subshells is seen (Fig. 6, solid line). This is compared with the ε_2 curve of 3p-transitions as derived from the reflectance measurements[8] by a Kramers-Kronig analysis (Fig. 6, dashed line). By adjusting both curves with their energy scales at thresholds for 3p- and 2p-transitions, one recognizes obvious similarities in the position and width of peaks in both curves, while the 3p-spectrum drops more rapidly with increasing energy.

As the 3p valence band has a width of 1 eV (including spin orbit and crystal field splitting), the peaks are somewhat broader than those of the 2p spectrum. The relative adjustment of the 3p- and 2p-energy scales in Fig. 6 is in contrast to our former interpretation[8], where we have mainly considered the profiles of the 3p reflection exciton peaks. However, the Kramers-Kronig transformation of

the 3p reflection data into ε_2 leads to a different shape of the 3p curve near the onset. Furthermore, the newer 2p-transition measurements show more details than the previous results included in ref. 8.

The main feature of both spectra is the big maximum at about 1.8 eV above threshold and a shoulder at 2.5 eV, followed by a minimum near 3 eV. Another region of enhanced absorption is between 4 and 6 eV above threshold. This feature may be correlated with the band calculations of Rössler[25]. The maxima B and C (b and c) are probably due to transitions to the lowest conduction band maxima near L_6^+ and X_6^+. The following maximum D corresponds to a transition into a flat conduction band part near Γ_8^+, which is 4.2 eV above the conduction band minimum at Γ_1^+. The peak A might correspond to transitions to critical points on the Δ- and Λ-line near 5 to 6 eV.

The agreement of our results with the calculations of Mattheis[20] and Lipari and Fowler[24] is not so good. Especially in the latter case there are no critical points in the conduction band which would correspond to the peaks at 1.8 eV and 2.5 eV above threshold.

ACKNOWLEDGEMENTS

The first preliminary results of the 2p-absorption in gaseous and solid Ar were obtained together with C. Kunz. The authors are grateful to U. Rössler and N.O. Lipari for sending them their band calculations prior to publications and to E.E. Koch, U. Rössler and M. Skibowski for stimulating discussions. Thanks are also due to the Deutsche Forschungsgemeinschaft for financial support.

LITERATURE

1) G.L. Pollack, Rev. Mod. Phys. 36, 748 (1964)

2) R.A. Guyer, in Solid State Physics Vol. 23, edited by F. Seitz, D. Turnbull and H. Ehrenreich (Academic Press Inc., New York and London, 1969), p 413

3) O. Schnepp and K. Dressler, J. Chem. Phys. 33, 49 (1960)

4) G. Baldini, Phys. Rev. 128, 1562 (1962)

5) I.T. Steinberger and O. Schnepp, Sol. State Comm. 5, 417 (1967)

6) J.F. O'Brien and K.J. Teegarden, Phys. Rev. Letters 17, 919 (1966)

7) D. Beaglehole, Phys. Rev. Letters 15, 551 (1965)

8) R. Haensel, G. Keitel, E.E. Koch, M. Skibowski and P. Schreiber, Phys. Rev. Letters 23, 1160 (1969)

9) I.T. Steinberger, C. Atluri and O. Schnepp, J. Chem. Phys. 52, 2723 (1970)

10) R. Haensel, G. Keitel, E.E. Koch, M. Skibowski and P. Schreiber, Opt. Comm. 2, 59 (1970)

11) R. Haensel, G. Keitel, E.E. Koch, N. Kosuch and M. Skibowski (to be published)

12) E.M. Hörl and J.A. Suddeth, J. Appl. Phys. 32, 2521 (1961)

13) H. Boersch, O. Bostanjoglo and L. Schmidt, Tagung für Elektronenmikroskopie, Aachen, 1965 (unpublished)

14) P. Keil, Z. Naturf. 21a, 503 (1966)

15) P. Keil, Z. Physik 214, 251 (1968)

16) C.E. Moore, Ntl. Bur. Std. (U.S.) Circ. No. 467 (U.S. GPO Washington, D.C.), Vol. I (1949); Vol. II (1958), Vol. III (1958)

17) R.S. Knox, The Theory of Excitons (Academic Press, Inc., New York and London, 1963)

18) R.S. Knox and F. Bassani, Phys. Rev. 124, 652 (1961)

19) W.B. Fowler, Phys. Rev. 132, 1591 (1963)

20) L.F. Mattheis, Phys. Rev. 133, A 1399 (1964)

21) M.H. Reilly, J. Phys. Chem. Sol. 28, 2067 (1967)

22) R. Ramirez and L.M. Falicov, Phys. Rev. B 1, 3464 (1970)

23) N.O. Lipari (to be published)

24) N.O. Lipari and W.B. Fowler (to be published)

25) U. Rössler (to be published)

26) R.P. Madden and K. Codling, in Autoionization; Astrophysical, Theoretical and Laboratory Experimental Aspects, edited by A. Temkin (Mono Book Corporation, Baltimore, Md., 1966), p 129

27) K. Codling, R.P. Madden and D.L. Ederer, Phys. Rev. 155, 26 (1967)

28) R.P. Madden, D.L. Ederer and K. Codling, Phys. Rev. 177, 136 (1969)

29) E.J. McGuire, Phys. Rev. 175, 20 (1968)

30) S.T. Manson and J.W. Cooper, Phys. Rev. 165, 126 (1968)

31) U. Fano and J.W. Cooper, Rev. Mod. Phys. 40, 441 (1968)

32) R. Haensel, G. Keitel, P. Schreiber and C. Kunz, Phys. Rev. Letters 22, 398 (1969)

33) R. Haensel, G. Keitel, P. Schreiber and C. Kunz, Phys. Rev. 188, 1375 (1969)

34) P. Schreiber, Dissertation Universität Hamburg 1970 (internal report DESY F41-70/5)

35) R. Haensel, G. Keitel, C. Kunz and P. Schreiber, Phys. Rev. Letters 25, 208 (1970)

36) R. Haensel and C. Kunz, Z. Ange. Phys. 23, 276 (1967)

37) R.P. Godwin, in Springer Tracts in Modern Physics, edited by G. Höhler (Springer Verlag, Berlin, 1969), Vol. 51, p. 1

38) J.A.R. Samson, Techniques of Vacuum Ultraviolet Spectroscopy (John Wiley & Sons, Inc., New York, 1967)

39) H. Wöhl, Diplomarbeit Universität Hamburg, 1968 (unpublished)

40) J.A.R. Samson, J. Opt. Soc. Am. 55, 935 (1965)

41) F.J. Comes and A. Elzer, Z. Naturf. 19a, 721 (1964)

42) D.L. Ederer and D.H. Tomboulian, Phys. Rev. 133, A 1525 (1964)

43) E. Dershem and M. Schein, Phys. Rev. 37, 1238 (1931)

44) B.L. Henke, R. White and B. Lundberg, J. Appl. Phys. 28, 98 (1957)

45) A.P. Lukirskii and T.M. Zimkina, Izv. Akad. Nauk. SSSR Ser. Fiz. 27, 817 (1963) (English transl.: Bull. Acad. Sci. USSR, Phys. Ser. 27, 808 (1963)).

46) R.D. Deslattes, Phys. Rev. 186, 1 (1969)

47) J.A.R. Samson, J. Opt. Soc. Am. 54, 420 (1964)

48) Po Lee and G.L. Weissler, Phys. Rev. 99, 540 (1955)

49) R.W. Alexander, D.L. Ederer and D.H. Tomboulian, Bull. Am. Phys. Soc. 9, 626 (1964)

50) Preliminary data which have been obtained in collaboration with C. Kunz are included in Ref. 8

51) W.S. Watson and F.J. Morgan, J. Phys. B 2, 277 (1969)

52) M. Nakamura, M. Sasanuma, S. Sato, M. Watanabe, H. Yamashita, Y. Iguchi, A. Ejiri, S. Nakai, S. Yamaguchi, T. Sagawa, Y. Nakai and T. Oshio, Phys. Rev. Letters 21, 1303 (1968)

53) A.P. Lukirskii and T.M. Zimkina, Izv. Akad. Nauk. SSSR Ser. Fiz. 27, 324 (1963) (English transl.: Bull. Acad. Sci. USSR Phys. Ser. 27, 333 (1963))

FIGURE CAPTIONS

Fig. 1 Experimental arrangement. EO = electron orbit, V = valve, SH = high energy radiation shielding, BS = beam shutter, CW = chopper wheel, Mo = monitor (Cu-Be sheet), F = filter, C = cryostat, M = mirror, ES = entrance slit of the Rowland monochromator, RA = rotating arm, G = grating, D = detector (photomultiplier behind the exit slit).

Fig. 2 Atomic cross section σ versus photon energy for solid and gaseous Ne in the energy range 25 - 400 eV. For comparison parts of the results of earlier measurements of Samson[40], Comes and Elzer[41], Ederer and Tomboulian[42], Dershem and Schein[43] and Henke et al.[44] are included.

Fig. 3 Atomic cross section σ versus photon energy for solid and gaseous Ar in the energy range 12 to 500 eV. The solid Ar data below 25 eV were deduced from ref. 8. For comparison parts of the results or earlier measurements of Lukirskii and Zimkina[45], Dershem and Schein[43], Henke et al.[44], Deslattes[46], Comes and Elzer[41], Samson[47], Po Lee and Weissler[48], Madden et al.[28] and Alexander et al.[49] are included.

Fig. 4 Absorption spectra of solid and gaseous Ne in the energy range 25 eV - 70 eV. The absolute values of the fine structure at 46 eV are fitted to Samson's data[40].

Fig. 5 Absorption spectra of solid and gaseous Ar in the energy range 242 - 272 eV. The identification of the gas absorption lines is given by Watson et al.[51] and Nakamura et al.[52]. In the solid the most important peaks are labeled with capital letters, unprimed and primed letters showing up spin-orbit pairs.

Fig. 6 Comparison of the ε_2-curve for 3p-transition in solid Ar (deduced from ref.8) (dashed line) with the absorption curve of 2p-transitions (solid line) unfolded for one subshell.

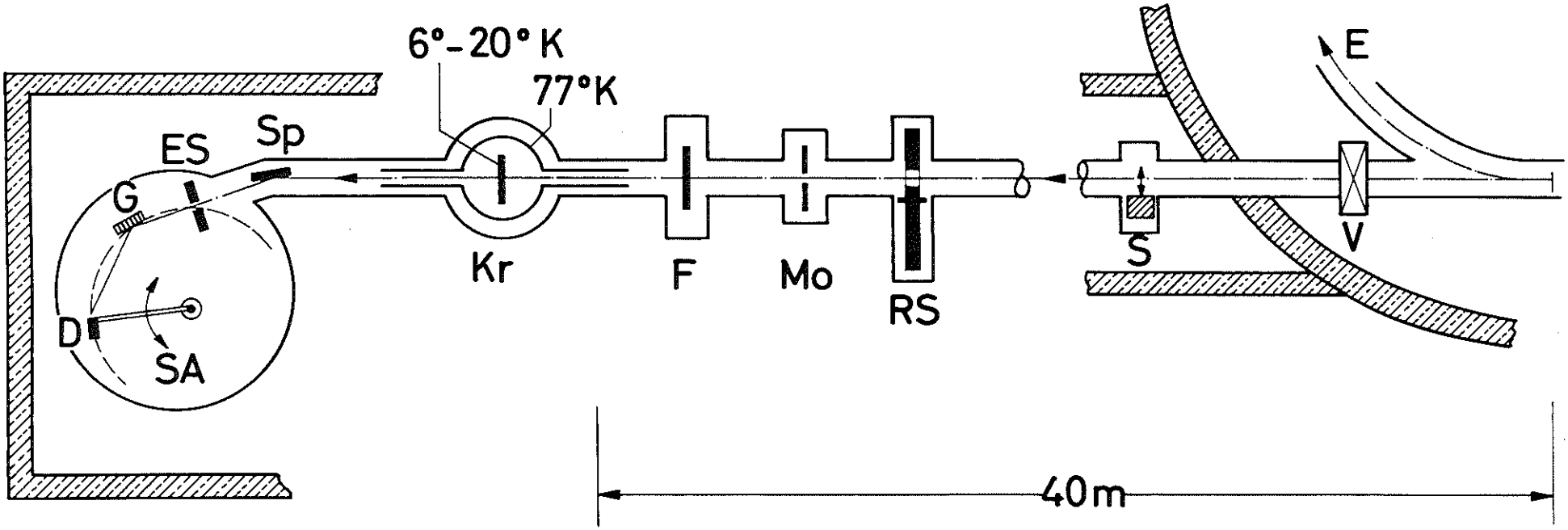

Fig.1

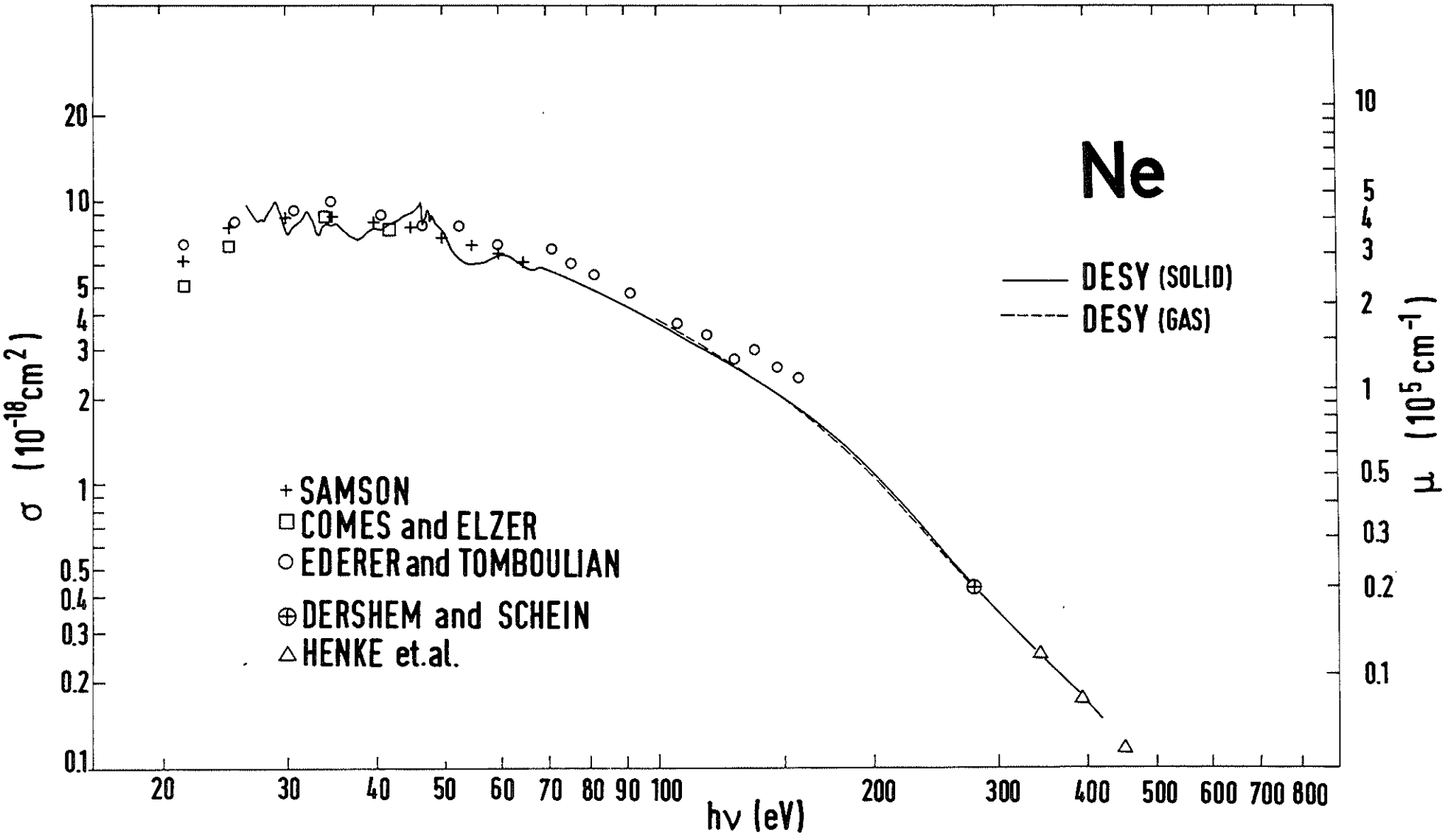
Ne
DESY (SOLID)
DESY (GAS)
+ SAMSON
□ COMES and ELZER
○ EDERER and TOMBOULIAN
⊕ DERSHEM and SCHEIN
△ HENKE et.al.
σ (10⁻¹⁸cm²)
μ (10⁵cm⁻¹)
hν (eV)
20
30
40
50
60
70
80
90
100
200
300
400
500
600
700
800
0.1
0.2
0.3
0.4
0.5
1
2
3
4
5
10

Fig.2

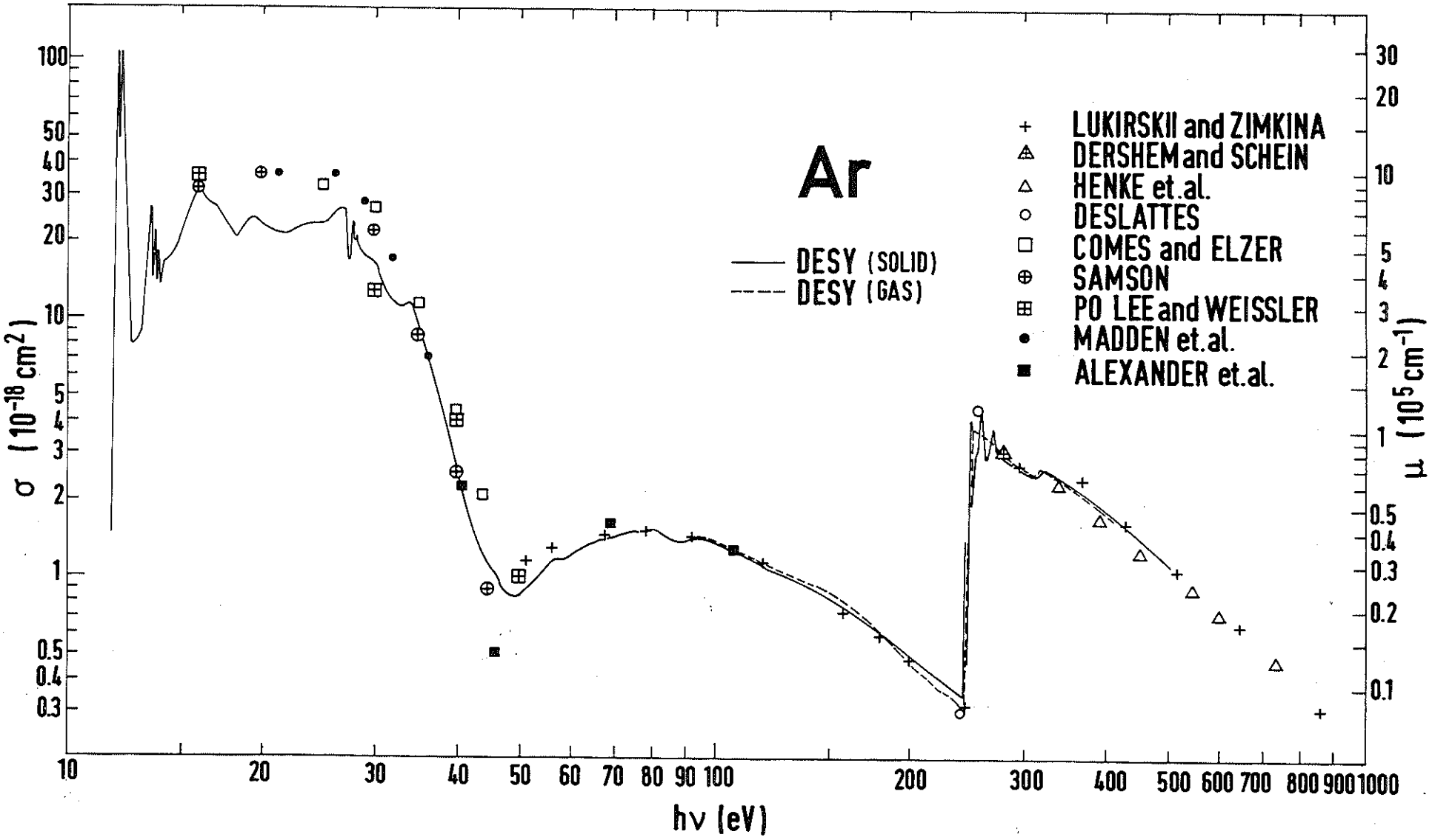
Ar
DESY (SOLID)
DESY (GAS)
LUKIRSKII and ZIMKINA
DERSHEM and SCHEIN
HENKE et.al.
DESLATTES
COMES and ELZER
SAMSON
PO LEE and WEISSLER
MADDEN et.al.
ALEXANDER et.al.
σ (10⁻¹⁸ cm²)
μ (10⁵ cm⁻¹)
hν (eV)

Fig.3

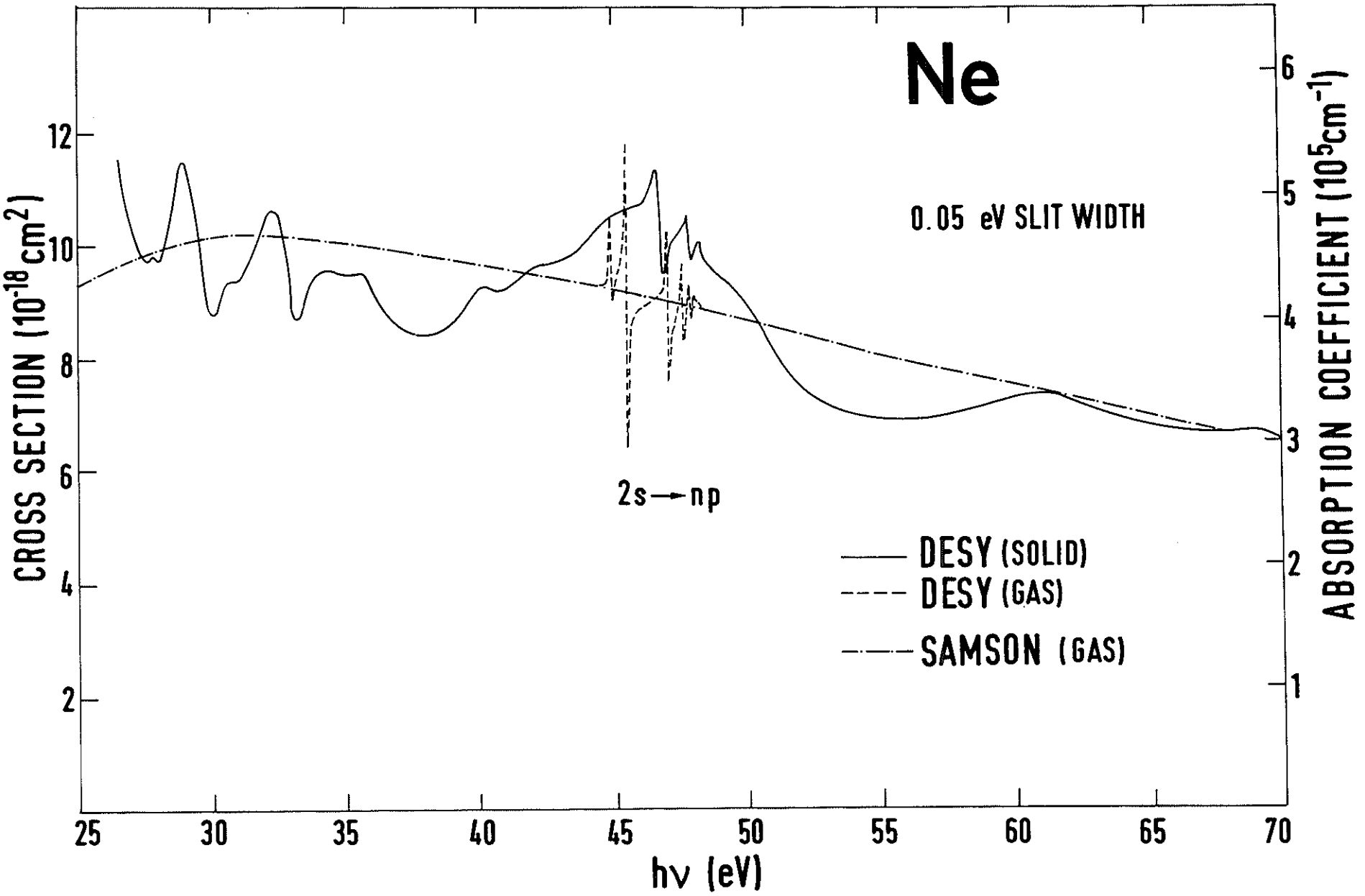
Ne
0.05 eV SLIT WIDTH
2s→np
DESY (SOLID)
DESY (GAS)
SAMSON (GAS)
CROSS SECTION (10^{-18}cm^2)
ABSORPTION COEFFICIENT (10^5cm^{-1})
hν (eV)
2
4
6
8
10
12
1
2
3
4
5
6
25
30
35
40
45
50
55
60
65
70

Fig.4

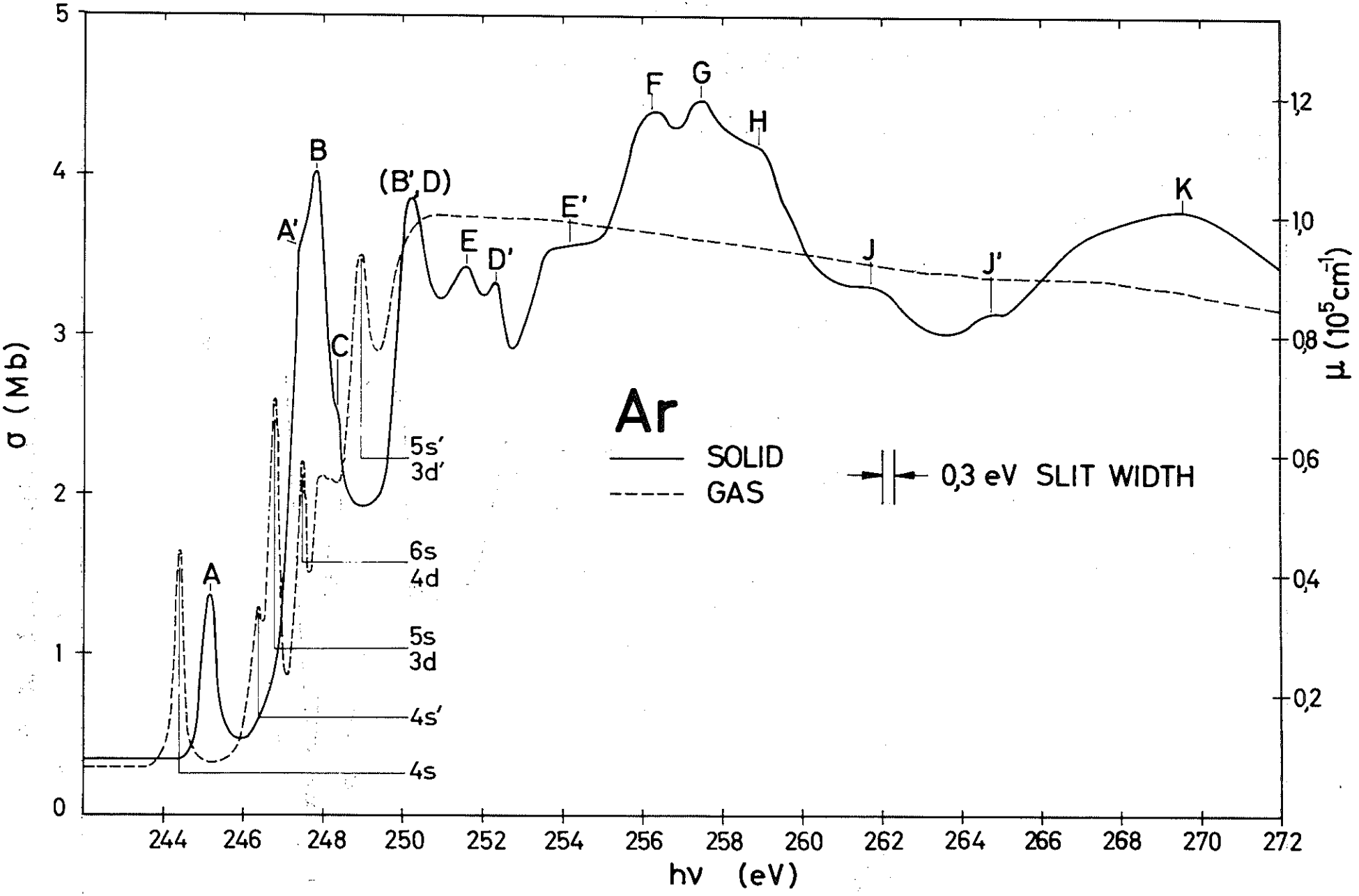
σ (Mb)
μ (10⁵cm⁻¹)
hν (eV)
Ar
SOLID
GAS
0,3 eV SLIT WIDTH
A
A'
B
C
(B',D)
D'
E
E'
F
G
H
J
J'
K
5s'
3d'
6s
4d
5s
3d
4s'
4s

Fig.5

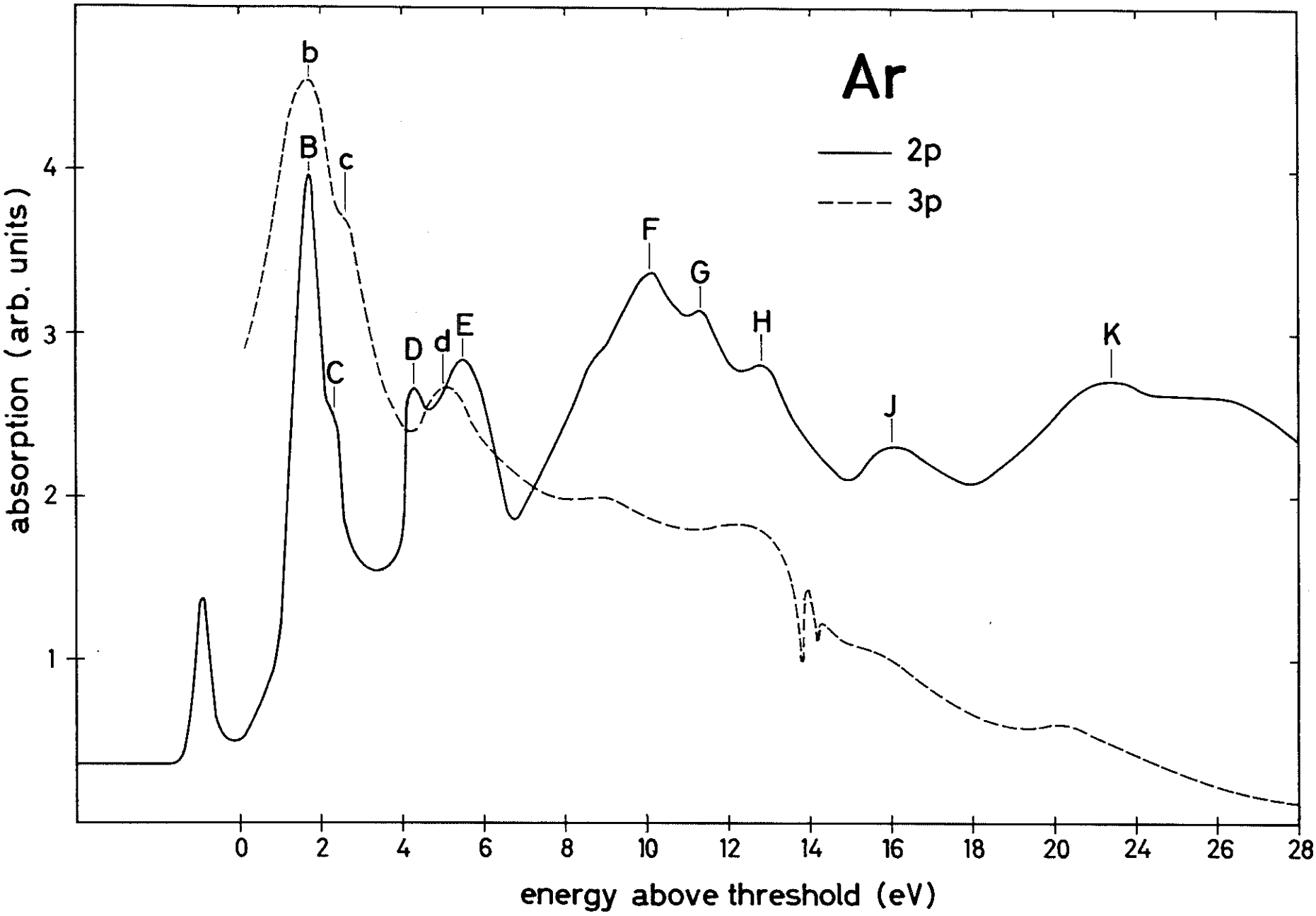
Ar
2p
3p
b
B
c
C
D
d
E
F
G
H
J
K
absorption (arb. units)
energy above threshold (eV)
1
2
3
4
0
2
4
6
8
10
12
14
16
18
20
24
26
28

Fig. 6